Pharmaceutical Nanotechnology

PLGA nanoparticles simultaneously loaded with vincristine sulfate and verapamil hydrochloride: Systematic study of particle size and drug entrapment efficiency

Xiangrong Song [a], Yu Zhao [b], Wenbin Wu [c], Yueqi Bi [a], Zheng Cai [a],
Qiuhong Chen [a], Yuanbo Li [a], Shixiang Hou [a,*]

[a] *West China School of Pharmacy, Sichuan University, No. 17, Section 3, Renmin Nan Road,
Chengdu, Sichuan 610041, PR China*
[b] *Department of Central Nervous System, Sanofi-Aventis, Room 3208 Office Building Plaza 66, No.1266,
Nanjing West Road, Shanghai 200040, PR China*
[c] *Department of Neurology, Sichuan Medical Science Academy and Sichuan Provincial People's Hospital,
No. 32, Section 2, Yihuan Road West, Chengdu, Sichuan 610072, PR China*

Abstract

PLGA nanoparticles simultaneously loaded with vincristine sulfate (VCR) and verapamil hydrochloride (VRP) were prepared via combining O/W emulsion solvent evaporation and salting-out method. Ten independent processing parameters and two materials characteristics were assessed systematically to enhance the incorporation of the two hydrophilic low molecular weight drugs into PLGA nanoparticles and minimize nanoparticles size. Approaches investigated for the enhancement of drug entrapment efficiencies and the minimization of particle size included the influence of the molecular weight (MW) of PLGA and the lactide to glycolide (L:G) ratio of PLGA, PLGA concentration, the degrees of hydrolyzation and polymerization of PVA, PVA concentration, initial VCR and VRP content, acetone to dichloromethane volume ratio, aqueous phase pH, salt concentration of aqueous phase, aqueous to organic phase volume ratio, sonication time, sonication energy and removal rate of organic solvents. The nanoparticles produced by optimal formulation were submicron size (111.4 ± 2.35 nm, $n = 3$) and of low polydispersity (0.062 ± 0.023, $n = 3$). Nanoparticles observed by transmission electron microscopy (TEM) showed extremely spherical shape. The entrapment efficiencies determined with high performance liquid chromatogram (HPLC) by ultracentrifuge method were $55.35 \pm 4.22\%$ for VCR and $69.47 \pm 5.34\%$ for VRP, respectively ($n = 3$).
© 2007 Elsevier B.V. All rights reserved.

Keywords: Vincristine sulfate; Verapamil hydrochloride; PLGA; Nanoparticles; O/W; Salting-out

1. Introduction

Resistance to chemotherapeutic drugs is one of the major problems in the treatment of cancer. Vincristine sulfate (VCR) is an effective chemotherapeutic agent, which has been used extensively for treatment of various cancers including AIDS-KS (Rowinsky and Donhower, 1996). Unfortunately, many tumor cells are not sensitive to VCR because of efflux from the tumor cells mediated by P-glycoprotein (Pgp), multidrug resistance-associated protein 1 (MRP1), MRP2 and MRP3 (Ambudkar et al., 2003; Borst et al., 2006). Overexpression of Pgp encoded by the MDR1 gene is one of the major obstacles to successful cancer therapy with VCR (Barthomeuf et al., 2005). Verapamil hydrochloride (VRP), a calcium channel blocker, has been reported to be able to reverse completely the resistance caused by Pgp in vitro at concentrations of approximately 5–10 μM (Huang et al., 1999). However, severe cardiovascular toxicity was observed when VRP plasma concentration reaches 1–2 μM in vivo (Ozofs et al., 1987). Meanwhile, VCR also has severe nervous system toxicity when administered systemically (Marinina et al., 2000). One way to decrease the toxicity of VRP and VCR is encapsulating them in nanoparticles that are capable of target-

---

ing tumor tissues or cells and changing their in vivo distributive characteristics. Julia et al. (1994) found that the administering sequence of antitumor agent and reversion agent would affect the efficacy of resistance reversion. Our previous research also proved that simultaneous administration of VCR and VRP could result in better treatment efficacy. Thus, it may be preferable to prepare nanoparticles incorporated with both VCR and VRP so that the two substances could be delivered simultaneously.

In this study, biodegradable nanoparticles made from Poly(d,l-lactide-co-glycolide acid) (PLGA), which have been extensively used as drug delivery systems for a variety of drugs (Jain, 2000; Vert, 1996), was chosen as carriers. In recent two decades, PLGA has attracted considerable attention and interest due to its excellent biocompatibility and biodegradability (Jain, 2000). Current literature is replete with studies investigating hydrophobic drug incorporation into PLGA nanoparticles (Budhian et al., 2007; Teixeira et al., 2005). It is relatively easier to entrap hydrophobic drugs into PLGA nanoparticles due to the hydrophobic nature of PLGA molecule. However, preparing hydrophilic drug loaded PLGA nanoparticles with high drug entrapment efficiency using the adapted preparation method represents a real challenge. Most reports concerning preparing hydrophilic drug loaded PLGA nanoparticles focused on the incorporation of macromolecules into PLGA nanoparticles, such as proteins and peptides (Choi and Park, 2006; Chong et al., 2005; Lamprecht et al., 2000), while PLGA nanoparticles loaded with low molecular weight drug were reported scarcely. Some of the common reported preparation methods of nanoparticles loaded with low molecular weight drug include nanoprecipitation (Barichello et al., 1999; Bilati et al., 2005), O/W single emulsification (Saxena et al., 2004; Tewes et al., 2007), W/O single emulsification (Niwa et al., 1995) and W/O/W double emulsification (Dillen et al., 2006; Tewes et al., 2007, Ubrich et al., 2004). Among them, the O/W single emulsification is the most difficult method to achieve a high entrapment efficiency, only Saxena et al. (2004) successfully prepared doxorubicin loaded PLGA nanoparticles with 95% entrapment efficiency using its neutral molecular form.

Taking into account of this information, the main aim of this study was to optimize the incorporation of two hydrophilic drugs (VCR and VRP) into PLGA nanoparticles by O/W single emulsification method to produce enhanced drug entrapment efficiency. The formulation parameters were systematically investigated. Thus, nanoparticles with some expectable properties such as high drug entrapment efficiency and small size can be produced through the optimized formulation. Following that, the physicochemical characteristics were also evaluated, which can provide some useful and essential information for in vitro cell experiments and in vivo studies.

2. Materials and methods

2.1. Materials

Different types of PLGA (shown in Fig. 1A) were purchased from Department of medical polymers Shandong institute, China. Six grades of Polyvinyl alcohol (PVA) with different

degrees of hydrolyzation and polymerization (shown in Fig. 1C) were purchased from Kuraray co., Ltd., China. VCR was purchased from Huanye Pharmaceutical Co., Ltd. (Guangzhou, China). VRP was obtained from Central Pharmaceutical Co., Ltd. (Tianjin, China). All other chemicals and solvents were of reagent grade.

2.2. Nanoparticle preparation

PLGA nanoparticles loaded with VCR and VRP were prepared using a modified version of an o/w single emulsion solvent evaporation process (Niwa et al., 1993; Niwa et al., 1994). The organic phase consisted of PLGA polymer and drugs dissolved in an acetone-dichloromethane mixture. The aqueous phase contained PVA solution. The organic phase was emulsified with the aqueous phase by sonication using a microtip probe sonicator (JY88-II ultrasonic processor, China) in ice bath. The organic mixture was then removed by evaporation leaving behind a colloidal suspension of PLGA nanoparticles (VV-PLGA-NPs) in water.

In this study, the effect of various processing parameters and polymer characteristics on nanoparticles mean diameter and drug entrapment efficiencies were assessed, including the molecular weight (MW) of PLGA and the lactide to glycolide (L:G) ratio of PLGA, PLGA concentration in the organic phase, the degrees of hydrolyzation (HD) and polymerization (PD) of PVA, PVA concentration in the aqueous phase, initial VCR and VRP content, acetone to dichloromethane (A/D) volume ratio, aqueous phase pH, salt concentration of aqueous phase, aqueous to organic phase (W/O) volume ratio, sonication time, sonication energy and removal rate of organic solvents. Unless otherwise mentioned, all the experiments were conducted by varying one of the parameters while keeping all the other process parameters at a set of standard conditions: 20 mg/ml of PLGA 50:50, MW 15 kDa, 54 μM of VCR and 20 mM of VRP in 1.5 ml of acetone-dichloromethane mixture (1:2, v/v) as the organic phase, and 4.5 ml of 1% PVA205 solution as the aqueous phase. The aqueous to organic phase volume ratio was 3:1 and polymer to drug ratio was 2:1 (PLGA/VRP, w/w). The time of sonication was 30 s at 50 W. The organic mixture was rapidly evaporated under reduced pressure at 37 °C. All batches of nanoparticles were produced at least in triplicate.

2.3. Determination of VCR and VRP entrapment efficiencies

To separate the soluble VCR and VRP in the supernatant from the nanoparticles, the nanoparticles suspension was ultra-centrifuged for 1 h at 4 °C at 223 000 × g (Optima MAX-E Ultracentrifuge, Beckman Coulter Inc., USA). The supernatant was removed and nanoparticles sediments were washed twice with water in order to remove the adsorbed drugs. The washing solution was eliminated by a further centrifugation as described above. And then, 5 ml of acetonitrile were added into the sediments and the mixture was vortexed for 5 min. After centrifugation at 76 × g (TGL-16G Centrifuge, Anting Scientific Apparatus Co., Ltd., Shanghai, China) for 10 min, 20 μl of super-
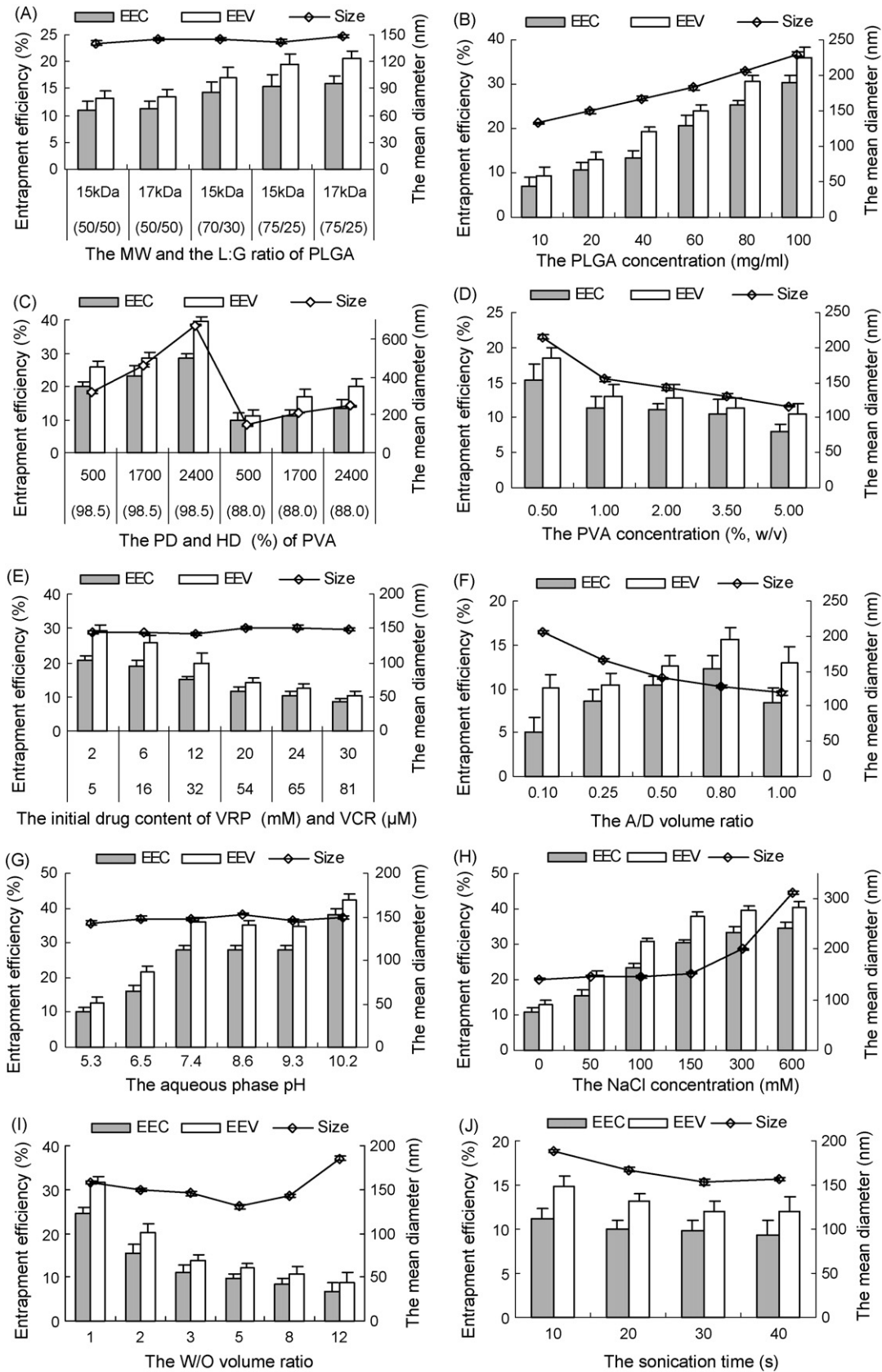
Fig. 1. Effect of various processing parameters and polymer characteristics on the mean diameter and drug entrapment efficiencies of nanoparticles, including the MW of PLGA and the L:G ratio of PLGA(A), PLGA concentration in the organic phase (B), the HD and PD of PVA (C), PVA concentration in the aqueous phase (D), initial VCR and VRP content (E), A/D volume ratio (F), aqueous phase pH (G), salt concentration of aqueous phase (H), W/O volume ratio (I), sonication time (J), sonication energy (K) and removal rate of organic solvents (L) ($n = 3$). The abbreviations of the entrapment efficiency of VCR and VRP are EEC and EEV, respectively.
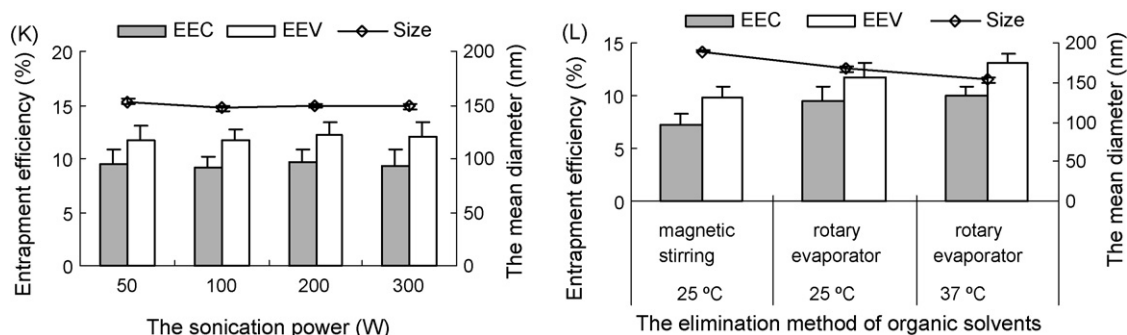
Fig. 1. (*Continued*).

natant was injected into an Agillent 1100 liquid chromatograph to determine the actual amounts of VCR and VRP incorporated within the nanoparticles. Separation was achieved using a Diamonsil C18 column (250 mm × 4.6 mm, 5 μm, Dikma Technologies, Beijing, China) at a flow rate of 1.0 ml/min and a detection of 278 nm. All the analysis was performed at 37 °C. To determine the total amount of VCR and VRP in the nanoparticles suspension, 500 μl of nanoparticles suspension was mixed with 4.5 ml of acetonitrile for 5 min by sonication. After centrifugation at $76 \times g$ for 10 min, supernatant was determined by HPLC analysis.

The entrapment efficiencies of VCR and VRP could be calculated with the percent ratio of the actual amounts of VCR and VRP incorporated into nanoparticles to the total amounts of VCR and VRP in nanoparticles suspension. Experiments were performed in triplicate.

2.4. Particle size and zeta potential

Particle size and polydispersity index were determined by photon correlation spectroscopy (PCS) using Zetasizer Nano ZS90 (Malvern Instruments Ltd., Malvern, UK). Size measurements were performed in triplicate following a 1/100 (v/v) dilution of the nanoparticles suspension in distilled water at 25 °C. The polydispersity index range was comprised between 0 and 1. Zeta potential was measured using the same instrument at 25 °C following the same dilution in an 1 mM NaCl solution. Each measurement was done in triplicate.

2.5. Transmission electron microscopy (TEM)

The morphology of the VV-PLGA-NPs was examined by TEM (H-600, Hitachi, Japan). Before analysis, the samples were diluted 1:5 and stained with 2% (w/v) phosphotungstic acid for 30 s and placed on copper grids with films for observation.

2.6. Data analysis

Multivariate data analysis was performed by multiple linear regression on Statistical Product and Service Solutions (SPSS V13.0, SPSS Inc., Chicago, USA).

3. Results and discussion

3.1. Effect of preparation variables on formulation characteristics

3.1.1. Factors affecting the mean diameter of VV-PLGA-NPs

In this study, the effect of 14 preparation variables on the mean diameter of VV-PLGA-NPs was investigated. The results are shown in Fig. 1 (A∼L). The mean diameter of VV-PLGA-NPs increased with the increase of MW of PLGA, PLGA concentration, HD of PVA, PD of PVA and NaCl concentration, but decreased with the increase of PVA concentration, A/D volume ratio, sonication time and removal rate of organic solvents. From Table 1, we could conclude that L:G ratio of PLGA, initial drugs content, aqueous phase pH and sonication power had no significant effect on the mean diameter. The results of statistical analysis showed that PLGA concentration, HD of PVA, PD of PVA, A/D volume ratio and NaCl concentration were the dominant factors ($p < 0.05$, respectively) in controlling the particle size.

Table 1
The relationship of various formulation parameters with the mean diameter and drug entrapment efficiencies of nanoparticles

Formulation parameters	Mean diameter	Entrapment efficiencies	
		VCR	VRP
MW of PLGA	+	+	+
L:G ratio of PLGA	0	+	+
PLGA concentration	+*	+*	+*
HD of PVA	+*	+*	+*
PD of PVA	+*	+	+
PVA concentration	−	−	−
Initial drugs content	0	−*	−*
A/D volume ratio	−*	+ −	+ −
Aqueous phase pH	0	+*	+*
NaCl concentration	+*	+*	+*
W/O volume ratio	− +	−*	−*
Sonication time	−	−	−
Sonication power	0	0	0
Removal rate of organic solvents	−	+	+

+ means positive correlation, − means negative correlation, 0 means no correlation, * means significance ($p < 0.05$).

Fig. 1A shows that the mean diameter increased slightly with the increase of MW of PLGA, which was in accordance with the result reported by Budhian et al. (2007). This phenomenon was probably resulted from the increase of the viscosity of internal phase, thereby decreasing the net shear stress and increasing the particle size.

Fig. 1B shows that the mean diameter of nanoparticles increased dramatically with the increase of PLGA concentration ($p < 0.05$). Increase in PLGA concentration leaded to the increase of the viscosity of the organic phase, thereby reducing the net shear stress and promoting the formation of droplets with larger size. In addition, the increasing viscosity could hinder rapid dispersion of PLGA solution into the aqueous phase, resulting in larger droplets which formed larger nanoparticles after elimination of the organic solvent. Moreover, with the increase of the amount of PLGA, PVA was probably insufficient to cover the surface of droplets completely, which caused the coalescence of droplets during the evaporation of organic solvent and aggregation of nanoparticles after the removal of organic solvent.

PVA grades could affect the mean diameter of nanoparticles significantly (Murakami et al., 1997). As HD and PD of PVA increased, the mean diameter of nanoparticles increased dramatically (Fig. 1C) ($p < 0.05$, respectively). PVA with high HD contained a large number of hydroxyl groups which could form hydrogen bonds between intra- or inter- molecules. The stronger intramolecular interaction via hydrogen bonds resulted in an increase of the aqueous phase viscosity (Hong et al., 2001; Lewandowska et al., 2001; Li et al., 2000; Lyoo et al., 2003), which leaded to an increase in particle size due to the reduction of the net shear stress available for droplet breakdown at a constant energy output. Meanwhile, the strong intermolecular interaction of hydroxyl groups adhering to the NP surface might result in coalescence of nanoparticles, thereby increasing the mean diameter of nanoparticles. Murakami et al. (1997) reported a decrease in size of PLGA nanoparticles at high HD of PVA, which was different from the outcome of this study. This contradiction could be elucidated because they measured the size after removing aggregates by passing through a 1.0-μm membrane filter, while we did not eliminate the aggregate. Increasing the PD of PVA also contributed to increase in viscosity of continuous phase, thereby resulting in larger nanoparticles. In contrast, increase in PVA concentration caused decrease of the mean diameter (Fig. 1D), which was in accordance with the result reported by Sahoo et al. (2002). At high concentration, more PVA can be oriented at organic solvent/water interface to reduce efficiently the interfacial tension (Galindo-Rodriguez et al., 2004), which resulted in significant increase in the net shear stress at a constant energy density (Nandi et al., 2001; Tesch and Schubert, 2002) during emulsification and promoted the formation of smaller emulsion droplets. Thus, the mean diameter of nanoparticles decreased with the increase of PVA concentration. However, with the increase in PVA concentration, the viscosity of the external aqueous phase increased, which resulted in size increase due to decrease in the net shear stress (Budhian et al., 2007). The change in the mean diameter with PVA concentration in this study was predominantly a result of reduction of the inter-

facial tension which dominated over the increasing viscosity. At high concentration, the amount of PVA was sufficient to cover the emulsion droplets completely. Therefore, during the removal of organic solvent, PVA can avoid the coalescence of droplets and then cause the formation of nanoparticles with smaller size. After the removal of organic solvent, more PVA molecules can be physically incorporated onto the NP surface (Boury et al., 1995; Galindo-Rodriguez et al., 2004), and then a large number of hydroxyl groups extending into the continuous phase could be hydrated, hence forming a hydrated layer at the surface to hinder nanoparticles aggregation.

Fig. 1F shows that nanoparticles mean diameter dramatically decreased with A/D volume ratio increasing ($p < 0.05$), which was consistent with literatures (Niwa et al., 1993; Niwa et al., 1994). The rapid dispersion of considerable amount of acetone into the external aqueous phase contributed to a significant reduction of the interfacial tension, thereby decreasing the particle size.

Fig. 1H shows that the mean diameter increased slightly with NaCl concentration increasing till 150 mM and then increased dramatically with the further increase of NaCl concentration ($p < 0.05$), which demonstrated that NaCl can change the viscosity of the external aqueous phase and thereby caused the change of nanoparticles size. In the concentration range from zero mM to 150 mM, NaCl had no substantial influence on the viscosity of the aqueous phase, while in the concentration range of 300–600 mM for NaCl, the viscosity of the aqueous phase increased dramatically, which resulted in significant increase in particle size.

Fig. 1I shows that the mean diameter first decreased and then increased with increase in W/O volume ratio. As W/O volume ratio increased, the amount of PVA increased, resulting in reduction of interfacial tension and thereby decreasing the nanoparticle size, as discussed above. On the other hand, the increasing volume of system would reduce the net shear stress due to a constant external energy input, leading to increase of size (Mainardes and Evangelista, 2005). The particle size was determined by the two competing effect of W/O volume ratio, namely, the mean size first decreased because the former dominated over the latter and then increased because the latter dominated over the former.

Fig. 1J shows that the mean diameter first decreased and then reached a plateau with the increase in sonication time, which was similar to the results reported in literatures (Kwon et al., 2001; Mainardes and Evangelista, 2005). With the larger time of sonication (30 s), the highest energy released in emulsification process, leading to the formation of smaller nanodroplets which were directly related to the final size of nanoparticles. In contrast, Fig. 1K shows that the sonication power was likely to have no effect on the mean diameter. That was probably because the sonication energy at 30w for 30s was sufficient enough to resist the interfacial tension. A further increase in sonication energy did not impact the size when sonication time was set at 30 s.

The removal rate of organic solvents had significant influence on nanoparticle size (Fig. 1L). As the removal rate of organic solvents increased, it was possible to eliminate the organic solvents in a shorter time, which could decrease coalescence and

aggregation of nanoparticles and hence decrease the mean diameter. This result was consistent with literatures (Lamprecht et al., 2001; Mainardes and Evangelista, 2005).

3.1.2. Variables influencing the drug entrapment efficiencies of VV-PLGA-NPs

The data of our previous cell experiment demonstrated that 10 μM of VRP can reverse completely the resistance of BEL-7402 (which only overexpressed Pgp) to 0.02 μM of VCR. The molar ratio of VCR to VRP in the above mentioned experiment was 1/500, but VCR had a slightly lower entrapment efficiency than VRP, so the molar ratio of VCR to VRP was fixed at 1/250 in the standard procedure.

As described in Fig. 1 (A~L) and Table 1, the change of entrapment efficiencies of VCR is coordinated with that of VRP. The entrapment efficiencies of the two drugs had a positive relationship with MW of PLGA, L:G ratio of PLGA, PLGA concentration, HD of PVA, PD of PVA, A/D volume ratio, aqueous phase pH, NaCl concentration and removal rate of organic solvents; and a negative relationship with PVA concentration, initial drugs content, W/O volume ratio and sonication time. Sonication power had no obvious influence on entrapment efficiencies of the two drugs. The results of multiple linear regression analysis illustrated that PLGA concentration, HD of PVA, initial drugs content, aqueous phase pH, NaCl concentration and W/O volume ratio were the main variables ($p < 0.05$, respectively) in generating particles entrapped with high amount of VCR and VRP.

The characteristics of PLGA can influence the entrapment of drugs (Fig. 1A). When the amount of lactide of PLGA increased, the interaction or affinity of both drugs with PLGA probably increased (Budhian et al., 2005; Seo et al., 2003), leading to increase in the entrapment efficiencies. When the MW of PLGA increased, the entrapment efficiencies of two drugs increased slightly, suggesting that the MW of PLGA may influence drugs incorporation, although it was reported that the MW of PLGA did not influence entrapment efficiency (Fonseca et al., 2002).

Increase in PLGA concentration leaded to a significant increase of the entrapment efficiencies of two drugs (Fig. 1B) ($p < 0.05$), which was probably resulted from the increase of viscosity. Increasing viscosity can increase the drugs resistance diffusional into the aqueous phase and thus increased the drugs incorporation into nanoparticles. Additionally, the increase of particle size may be relevant to the increase of drugs entrapment efficiencies (Budhian et al., 2007). The increase of nanoparticles size with the increasing PLGA concentration, can increase the length of diffusional pathways of drugs from the organic phase to the aqueous phase, thereby reducing the drug loss through diffusion and increasing the drugs entrapment efficiencies.

Increase in HD of PVA caused a significant increase of the entrapment efficiencies of two drugs (Fig. 1C) ($p < 0.05$), which was probably attributed to three aspects as follows. Firstly, increase in the HD of PVA leaded to the increase of viscosity of the aqueous phase, hence forming nanoparticles with large size. As discussed above, larger nanoparticles had higher drugs entrapment efficiencies. Secondly, the hydroxyl groups of PVA adsorbing onto the identical NP surface may form a thick film on
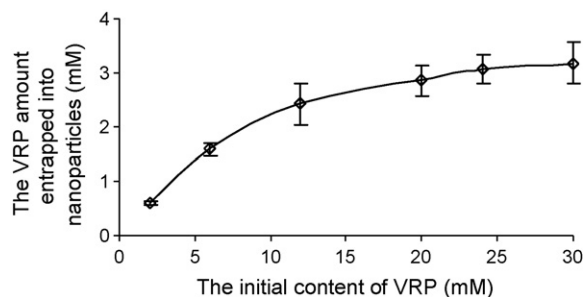

Fig. 2. Effect of initial VRP content on the amount of VRP entrapped into nanoparticles.

the NPs surface via the stronger intra- or inter- molecular interaction. The thick film possibly delayed the diffusion of drugs into the aqueous phase, thereby decreasing drug loss. Thirdly, the increase of viscosity decreased the rate of drug diffusion into the aqueous phase, thus increasing the entrapment efficiencies. Similarly, the high PD of PVA leaded to high entrapment efficiencies (Fig. 1C), which also was resulted from the large size of nanoparticles. In contrast, the entrapment efficiencies decreased with the increase of PVA concentration. That was probably caused by the decrease in particle size. Moreover, with the increase in PVA concentration, more molecules of two drugs may partition out rapidly into the aqueous phase during emulsification procedure and less drugs molecules remained in emulsion droplets to interact with PLGA molecules, hence decreasing the entrapment efficiencies.

The increase of the initial drugs content resulted in significant reduction in entrapment efficiencies of the two drugs ($p < 0.05$), which was possibly caused by the nonlinear increase in the amounts of VCR and VRP entrapped into nanoparticles, as shown in Figs. 2 and 3. With increase in initial content of two drugs, the concentration of drugs in the organic phase increased and then more drug molecules can interact with PLGA molecules, resulting in the increase of the entrapment amounts of VCR and VRP. Nevertheless, the increase of the entrapment amounts of drugs was not in proportion to the increase of initial drug content, thus the entrapment efficiencies decreased.

When A/D volume ratio increased, the mean entrapment efficiencies of two drugs first increased progressively and then decreased dramatically (Fig. 1F). This occurred possibly because the change of A/D volume ratio affected the partition of two drugs in the organic phase. In order to support the spec-
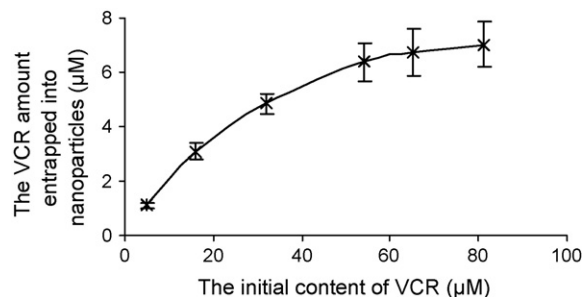

Fig. 3. Effect of initial VCR content on the amount of VCR entrapped into nanoparticles.
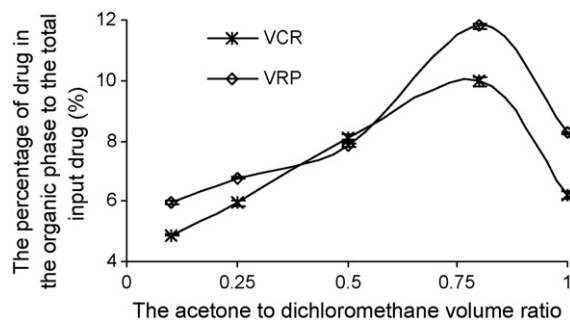
Fig. 4. Effect of the ratio of acetone to dichloromethane volume on the percentage of drug in the organic phase to the total input drug.

Fig. 5. Effect of NaCl concentration on the percentage of drug in the organic phase to the total input drug.

ulation, the partition of two drugs in the organic phase was investigated at five different ratios of A/D volume accordant with the ratios presented in Fig. 1F. The experiments were carried out as follows: the organic phase, consisting of constant drugs dissolved in 1.5 ml of acetone-dichloromethane mixture with different volume ratio, was mixed with 4.5 ml of aqueous phase without PVA by sonication in ice bath for 30s at 50W. Then the mixed solution was centrifuged at $76 \times g$ for 10 min, supernatant was collected for further HPLC analysis to determine the actual amount of VCR and VRP in the aqueous phase. Then the percentage of VCR and VRP in the organic phase to the total input drugs could be calculated. As described in Fig. 4, it was clear that the change in entrapment efficiencies of two drugs with A/D volume ratio was predominantly a result of changing amount of drugs in the organic phase.

The aqueous phase pH would affect the entrapment efficiencies of two drugs dramatically (Fig. 1G) ($p < 0.05$). VCR and VRP have a sulfate group and a hydrochloride group respectively, imparting hydrophilic character to the drugs molecules. Due to their water-solubility, lower entrapment efficiencies were obtained in this study. During emulsification and solvent evaporation process, drug molecules quickly partitioned out into the aqueous phase from the organic phase, hence causing extremely less VCR and VRP retention in the polymer matrix. In order to enhance the incorporation of the two water-soluble drugs, studies were subsequently performed using external phase with different pH values adjusted to with NaOH. The results are presented in Fig. 1G. The change trend of entrapment efficiencies with the increasing aqueous phase pH was similar to those reported by literatures (Govender et al., 1999; Song et al., 1997). As the aqueous phase pH increased, the entrapment efficiencies of two drugs first increased gradually, subsequently reached a plateau, and then maximized at pH 10.2. When the aqueous pH increases, the ionization degree of two drugs probably reduced (Govender et al., 1999) and then more drug molecules without ionization can be retained in the hydrophobic nanoparticle matrix, thereby increasing the drugs entrapment efficiencies. The higher entrapment efficiencies of two drugs were achieved at pH 10.2 as shown in Fig. 1G, whereas an aqueous medium with this alkaline pH could promote the degradation of PLGA and was unsuitable for intravenous injection. Therefore, pH 7.4 was selected as the optimal pH of the aqueous phase.
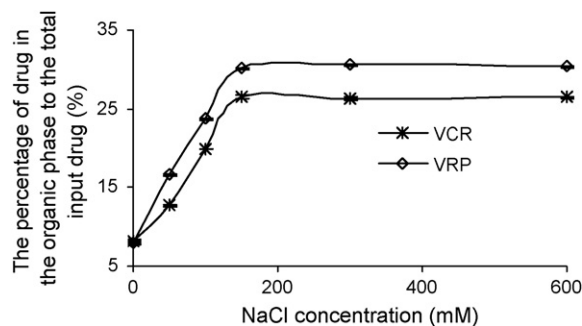
Combining the salting-out and the emulsion solvent evaporation method could further increase the entrapment efficiencies of two drugs. In this study, NaCl was selected as salting-out agent instead of CaCl$_2$ (Perugini et al., 2002) and MgCl$_2$ (Allemann et al., 1993), both of which would change the aqueous phase pH slightly. Fig. 1H shows that the entrapment efficiencies of two drugs first increased dramatically and then reached a plateau with a slight increase when NaCl concentration increased ($p < 0.05$), which did not agree well with the results reported by McCarron et al. (2006).The change of entrapment efficiencies with NaCl concentration was probably a result of changing partition of two drugs in the organic phase. The partition of two drugs in the organic phase was investigated at different NaCl concentration as described above. The results are shown in Fig. 5. The percentage of two drugs in the organic phase increased dramatically with the increase in NaCl concentration till 150 mM, which enabled more drug molecules to interact with PLGA molecules and thus enhanced drug incorporation into nanoparticles. Nevertheless, no further increase in the percentage was observed when NaCl concentration was beyond 150 mM. Therefore, the slight increase in entrapment efficiencies could be attributed to the increasing particle size when NaCl concentration was between 300 mM and 600 mM.

As shown in Fig. 1I, the mean entrapment efficiencies of two drugs decreased dramatically with the increase of W/O volume ratio ($p < 0.05$). This occurred because the amount of drugs partitioned into the organic phase reduced during emulsification, meanwhile, the drugs loss increased during solvent evaporation when the W/O volume ratio increased.

Increase in sonication time resulted in reduction in the mean entrapment efficiencies of two drugs (Fig. 1J) due to the decreasing size of nanoparticles as discussed above. While the sonication energy was likely to have no effect on the entrapment efficiencies of two drugs as presented in Fig. 1K because of no change in size.

Increase in the removal rate of organic solvents increased the entrapment efficiencies of two drugs (Fig. 1L). As the removal rate of organic solvents increased, it was possible to eliminate the organic solvents in a shorter time and minimize drug diffusion into the aqueous phase, thereby enhancing the drugs entrapment owing to the decrease of drugs loss.

3.2. Optimization of VV-PLGA-NPs

According to the results described above, higher entrapment efficiencies could be achieved when the salt concentration and pH of the aqueous phase was set at 150 mM and 7.4, respectively. In order to simplify the preparation process, pH 7.4 phosphate buffered solution (PBS) (300mM) was chosen instead of NaCl. To verify the optimal parameters, VV-PLGA-NPs were subsequently prepared as follows: 80 mg of PLGA (75:25, 15000), 54 μM of VCR and 20 mM of VRP were dissolved into 1.5 ml of acetone-dichloromethane (0.8/1, v/v), which formed organic phase. The organic phase was emulsified with 3 ml of pH 7.4 phosphate buffered solution containing PVA205 (2%, w/v) by probe sonication at 50 W for 30 s in ice bath. The organic solvent was then rapidly evaporated under reduced pressure at 37 °C.

3.3. Characterization of the optimal nanoparticle formulation

The optimized VV-PLGA-NPs improved significantly the drug incorporation, with an entrapment efficiency of $55.35 \pm 4.22\%$ for VCR and $69.47 \pm 5.34\%$ for VRP, respectively ($n = 3$). The molar ratio of VCR to VRP entrapped into nanoparticles was approximately 1/500, which might achieve a desirable efficacy in reversing resistance. VV-PLGA-NPs were characterized by PCS and exhibited a diameter of 107.4 ± 7.35 nm ($n = 3$). The polydispersity index of 0.062 ± 0.023 ($n = 3$) indicated a narrow size distribution. The PCS results of three batches of nanoparticles had no substantial difference, which demonstrated that the preparation process was reproducible and stable. TEM shows nanoparticles with a mean diameter of 65 nm, a spherical shape and a smooth surface (Fig. 6). The size of the VV-PLGA-NPs determined by PCS was not consistent with that of determined by TEM, which was probably caused by the different mechanisms of the two methods. PCS and TEM were based on scattering (hydrodynamic radius) and diffraction technique in particle size measurement, respectively. The size detection of VV-PLGA-NPs by PCS was carried out in aqueous state and in this case, nanoparticles were highly
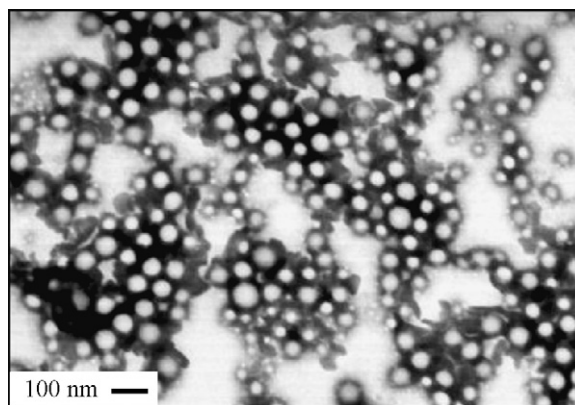

Fig. 6. Transmission electron micrograph of VV-PLGA-NPs, scale bar: 100 nm.

hydrated and the diameters detected by PCS were 'hydrated diameters', which are usually larger than their genuine diameters. In the case of TEM sample preparation, VV-PLGA-NPs were stained with 2% (w/v) phosphotungstic acid and all the free water and even some of hydrated water was stained. This implied that the sizes of VV-PLGA-NPs derived from TEM might be considerably smaller than their real diameters. The zeta potential of VV-PLGA-NPs (pH 7.4) was slightly negative, with the value of -0.75 ± 0.12 mV ($n = 3$).

4. Conclusion

In this paper, the influences of various processing variables on particle size and drug entrapment efficiencies were systematically assessed. It was concluded that formulation variables can be exploited in order to enhance the incorporation of a hydrophilic low molecular weight drug into PLGA nanoparticles by O/W single emulsification method. Based on the optimal parameters, it was found that VV-PLGA-NPs with expectable properties could be obtained through combining O/W emulsion solvent evaporation method and the salting-out method. This study has shown that two hydrophilic low molecular weight drugs, VCR and VRP, could be simultaneously entrapped into PLGA nanoparticles, with a relatively high entrapment effi-

Table 2

Optimization of formulation variables to control the size and drug entrapment efficiency of nanoparticles prepared by O/W emulsion solvent evaporation method based on scientific principles

Governing scientific principles	Pertinent formulation varibles
Small size	
Increase the net shear stress	Decrease W/O volume ratio
Decrease the viscocity	Increase applied energy during emulsification (power, duration)
Decrease the interface tension	Optimize PVA concentration, Increase A/D volume ratio, Optimize W/O volume ratio, Decrease MW of PLGA, Decrease PLGA concentration, Decrease HD of PVA, Decrease PD of PVA, Decrease the salt concentration in aqueous phase
Increase the stabilization role	Increase PVA concentration, Increase the removal rate of organic solvent, Decrease PLGA concentration
High entrapment efficiency	
Increase drug–polymer interaction	Optimize L:G ratio of PLGA, Sufficient initial drug content for specific interactions
Increase the partition of drug in organic phase	Increase the salt concentration in aqueous phase, Optimize A/D volume ratio
Inhibit drug diffusion during organic solvent evaporation	Increase particle size, Decrease relative volume of organic solvent
Longer diffusion path length, Shorter diffusion times, Increase resistance to diffusion, Reduce drug solubility in aqueous phase	Increase PLGA concentration, Optimize MW of PLGA, Increase the removal rate of organic solvent, Reduce drug solubility in the aqueous phase (alter pH)

ciency of $55.35 \pm 4.22\%$ for VCR and $69.47 \pm 5.34\%$ for VRP respectively and small size of around 110 nm.

Table 2 summarized how to optimize the formulation variables to control the size and drug entrapment efficiency of nanoparticles based on scientific principles, which could be applied to any hydrophilic-drug-polymer system produced by the simple modified O/W emulsion solvent evaporation method. This systematical investigation reported here might promote the development of more PLGA nanoparticles loaded with hydrophilic low molecular weight drug.

Acknowledgements

References

Allemann, E., Leroux, J.C., Gurny, R., Doelker, E., 1993. In vitro extended-release properties of drug-loaded poly (DL-lactic acid) nanoparticles produced by a salting-out procedure. Pharm. Res. 10, 1732–1737.

Ambudkar, S.V., Kimchi–Sarfaty, C., Sauna, Z.E., Gottesman, M.M., 2003. P-glycoprotein from genomics to mechanism. Oncogene 22, 7468–7485.

Barichello, J.M., Morishita, M., Takayama, K., Nagai, T., 1999. Encapsulation of hydrophilic and lipophilic drugs in PLGA nanoparticles by the nanoprecipitation method. Drug Dev. Ind. Pharm. 25, 471–476.

Barthomeuf, C., Grassi, J., Demeule, M., Fournier, C., Boivin, D., Beliveau, R., 2005. Inhibition of P–glycoprotein transport function and reversion of MDR1 multidrug resistance by cnidiadin. Cancer Chemother. Pharmacol. 56, 173–181.

Bilati, U., Allémann, E., Doelker, Eric, 2005. Development of a nanoprecipitation method intended for the entrapment of hydrophilic drugs into nanoparticles. Eur. J. Pharm. Sci. 24, 67–75.

Borst, P., Zelcer, N., van de Wetering, K., Poolman, B., 2006. On the putative co-transport of drugs by multidrug resistance proteins. FEBS Lett. 580, 1085–1093.

Boury, F., Ivanova, T., Panaiotov, I., Proust, J.E., Bois, A., Richou, J., 1995. Dynamic properties of poly(DL-lactide) and polyvinyl alcohol monolayers at the air/water and dichloromethane/water interfaces. J. Colloid Interface Sci. 169, 380–392.

Budhian, A., Siegel, S.J., Winey, K.I., 2005. Production of haloperidol-loaded PLGA nanoparticles for extended controlled drug release of haloperidol. J. Microencapsul. 22, 773–785.

Budhian, A., Siegel, S.J., Winey, K.I., 2007. Haloperidol-loaded PLGA nanoparticles: Systematic study of particle size and drug content. Int. J. Pharm. 336, 367–375.

Choi, S.H., Park, T.G., 2006. G-CSF loaded biodegradable PLGA nanoparticles prepared by a single oil-in-water emulsion method. Int. J. Pharm. 311, 223–228.

Chong, C.S.W., Cao, M., Wong, W.W., Fischer, K.P., Addison, W.R., Kwon, G.S., Tyrrell, D.L., Samuel, John., 2005. Enhancement of T helper type 1 immune responses against hepatitis B virus core antigen by PLGA nanoparticle vaccine delivery. J. Control. Release 102, 85–99.

Dillen, K., Vandervoort, J., Van den Mooter, G., Ludwig, A., 2006. Evaluation of ciprofloxacin-loaded Eudragit® RS100 or RL100/PLGA nanoparticles. Int. J. Pharm. 314, 72–82.

Fonseca, C., Simoes, S., Gaspar, R., 2002. Paclitaxel-loaded PLGA nanoparticles, preparation, physicochemical characterization and in vitro anti-tumoral activity. J. Control. Release 83, 273–286.

Galindo-Rodriguez, S., Allemann, E., Fessi, H., Doelker, E., 2004. Physicochemical parameters associated with nanoparticle formation in the salting-out, emulsification-diffusion and nanoprecipitation methods. Pharm. Res. 21, 1428–1439.

Govender, T., Stolnik, S., Garnett, M.C., Illum, L., Davis, S.S., 1999. PLGA nanoparticles prepared by nanoprecipitation, drug loading and release studies of a water soluble drug. J. Control. Release 57, 171–185.

Hong, P.D., Chou, C.M., He, C.H., 2001. Solvent effects on aggregation behavior of polyvinyl alcohol solutions. Polymer 42, 6105–6112.

Huang, M., Liu-G, T.I., Prat, F., Centarti, M., Sibille, E., 1999. The study of innate drug resistance of human hepatocellular carcinoma Bel7402 cell line. Cancer Letters 135, 97–105.

Jain, R.A., 2000. The manufacturing techniques of various drug loaded biodegradable poly(lactide–co–glycolide) (PLGA) devices. Biomaterials 21, 2475–2490.

Julia, A.M., Roche, H., Berlion, M., 1994. Multidrug resistance circumvention by a new triazi–noaminopiperidine derivative S9788 in vitro,definition of the optimal schedule and comparison with verapamil. Br. J. Cancer 69, 868–875.

Kwon, H.-Y., Lee, J.-Y., Choi, S.-W., Jang, Y., Kim, J.-H., 2001. Preparation of PLGA nanoparticles containing estrogen by emulsification-diffusion method. Colloid Surf. A 182, 123–130.

Lamprecht, A., Ubrich, N., Hombreiro Pérez, M., Lehr, C.-M., Hoffman, M., Maincent, P., 2000. Influences of process parameters on nanoparticle preparation performed by a double emulsion pressure homogenization technique. Int. J. Pharm. 196, 177–182.

Lamprecht, A., Ubrich, N., Yamamoto, H., Schafer, U., Takeuchi, H., Lehr, C.–M., Maincent, P., Kawashima, Y., 2001. Design of rolipram-loaded nanoparticles, comparison of two preparation methods. J. Control. Release 71, 297–306.

Lewandowska, K., Staszewska, D.U., Bohdanecky, M., 2001. The Huggins viscosity coefficient of aqueous solution of poly(vinyl alcohol). Eur. Polym. J. 37, 25–32.

Li, H., Zhang, W., Xu, W., Zhang, X., 2000. Hydrogen bonding governs the elastic properties of poly(vinyl alcohol) in water, singlemolecule force spectroscopic studies of PVA by AFM. Macromolecules 33, 465–469.

Lyoo, S.W., Seo, S.I., Ji, C.B., Kim, H.J., Kim, S.S., Ghim, D.H., Kim, C.B., Lee, J., 2003. Role of the stereosequences of poly(vinyl alcohol) in the rheological properties of syndiotacticity-rich poly-(vinyl alcohol)/water solutions. J. Appl. Polym. Sci. 88, 1858–1863.

Mainardes, R.M., Evangelista, R.C., 2005. PLGA nanoparticles containing praziquantel: effect of formulation variables on size distribution. Int. J. Pharm. 290, 137–144.

Marinina, J., Shenderova, A., Mallery, S.R., Schwendeman, S.P., 2000. Stabilization of vinca alkaloids encapsulated in poly(lactide-co-glycolide) microspheres. Pharma. Res. 17, 677–683.

McCarron, P.A., Donnelly, R.F., Marouf, W., 2006. Celecoxib-loaded poly(D,L-lactide-co-glycolide) nanoparticles prepared using a novel and controllable combination of diffusion and emulsification steps as part of the salting-out procedure. J. Microencapsul. 23, 480–498.

Murakami, H., Kawashima, Y., Niwa, T., Hino, T., Takeuchi, H., Kobayashi, M., 1997. Influence of the degrees of hydrolyzation and polymerization of poly(vinylalcohol) on the preparation and properties of poly(DL-lactide-co-glycolide) nanoparticle. Int. J. Pharm. 149, 43–49.

Nandi, A., Khakhar, D.V., Mehra, A., 2001. Coalescence in surfactant-stabilized emulsions subjected to shear flow. Langmuir 17, 2647–2655.

Niwa, T., Takeuchi, H., Hino, T., Kunou, N., Kawashima, Y., 1993. Preparations of biodegradable nanospheres of water-soluble and insoluble drugs with D,L-lactide/glycolide copolymer by a novel spontaneous emulsification solvent diffusion method, and the drug release behavior. J. Control. Release 25, 89–98.

Niwa, T., Takeuchi, H., Hino, T., Kunou, N., Kawashima, Y., 1994. In vitro drug release behavior of D, L-lactide/glycolide copolymer (PLGA) nanospheres with nafarelin acetate prepared by a novel spontaneous emulsification solvent diffusion method. J. Pharm. Sci. 83, 727–732.

Niwa, T., Takeuchi, H., Hino, T., Nohara, M., Kawashima, Y., 1995. Biodegradable submicron carriers for peptide drugs, preparation of DL-lactide/glycolide copolymer (PLGA) nanospheres with nafarelin acetate by a novel emulsion–phase separation method in an oil system. Int. J. Pharm. 121, 45–54.

Ozofs, R.F., Cunnion, R.E., Kfecker Jr., R.W., Hamilton, T.C., Ostchega, Y., Parriflo, J.E., Young, R.C., 1987. Verapamif and adriamycin in the treatment of drug-resistant ovarian cancer patients. J. Clin. Oncol. 5, 641–647.

Perugini, P., Simeoni, S., Scalia, S., Genta, I., Modena, T., Conti, B., Pavanetto, F., 2002. Effect of nanoparticle encapsulation on the photostability of the sunscreen agent, 2-ethylhexyl-p-methoxycinnamate. Int. J. Pharm. 246, 37–45.

Rowinsky, E., Donhower, R.C., 1996. Antimicrotubule agents. In: Chabner, B.A., Longo, D.L. (Eds.), Cancer Chemotherapy and Biotherapy. Lippincot-Raven Publishers, Philadelphia, pp. 263–275.

Saxena, V., Sadoqi, M., Shao, J., 2004. Indocyanine green-loaded biodegradable nanoparticles, preparation, physicochemical characterization and in vitro release. Int. J. Pharm. 278, 293–301.

Seo, S.A., Khang, G., Rhee, J.M., Kim, J., Lee, H.B., 2003. Study on in vitro release patterns of fentanyl-loaded PLGA microspheres. J. Microencapsul. 20, 569–579.

Song, C.X., Labhasetwar, V., Murphy, H., Qu, X., Humphrey, W.R., Shebuski, R.J., Levy, R.J., 1997. Formulation and characterisation of biodegradable nanoparticles for intravascular local drug delivery. J. Control. Release 43, 197–212.

Teixeira, M., Alonsoc, M.J., Pinto, M.M.M., Barbosa, C.M., 2005. Development and characterization of PLGA nanospheres and nanocapsules containing xanthone and 3–methoxyxanthone. Eur. J. Pharm. Biopharm. 59, 491–500.

Tesch, S., Schubert, H., 2002. Influence of increasing viscosity of the aqueous phase on the short-term stability of protein stabilized emulsions. J. Food Eng. 52, 305–312.

Tewes, F., Munnier, E., Antoon, B., Okassa, L.N., Cohen-Jonathan, S., Marchais, H., Douziech-Eyrolles, L., Soucé, M., Dubois, P., Chourpa, I., 2007. Comparative study of doxorubicin-loaded poly(lactide-co-glycolide) nanoparticles prepared by single and double emulsion methods. Eur. J. Pharm. Biopharm. 66, 488–492.

Ubrich, N., Bouillot, P., Pellerin, C., Hoffman, M., Maincent, P., 2004. Preparation and characterization of propranolol hydrochloride nanoparticles, a comparative study. J. Control. Release 97, 291–300.

Vert, M., 1996. The complexity of PLAGA–based drug delivery systems. In: Proceedings of the International Conference on Advances in Controlled Delivery, Baltimore, MD, pp. 32–36.